Current-voltage spectroscopy of the subband structure of strongly pinched-off quantum point contacts

J. Song, Y. Kawano, K. Ishibashi, J. Mikalopas, G. R. Aizin et al.

Citation: Appl. Phys. Lett. **95**, 233115 (2009); doi: 10.1063/1.3272677
View online: http://dx.doi.org/10.1063/1.3272677
View Table of Contents: http://apl.aip.org/resource/1/APPLAB/v95/i23
Published by the American Institute of Physics.

Current-voltage spectroscopy of the subband structure of strongly pinched-off quantum point contacts

J. Song,[1] Y. Kawano (河野行雄),[2] K. Ishibashi (石橋幸治),[2] J. Mikalopas,[3] G. R. Aizin,[3] N. Aoki (青木伸之),[4] J. L. Reno,[5] Y. Ochiai (落合勇一),[4] and J. P. Bird[1,4,a)]
[1]*Department of Electrical Engineering, University at Buffalo, The State University of New York, Buffalo, New York 14260-1920, USA*
[2]*Advanced Device Laboratory, The Institute of Physical and Chemical Research (RIKEN), 2-1, Hirosawa, Wako, Saitama 351-0198, Japan*
[3]*Department of Physical Sciences, Kingsborough College, City University of New York, Brooklyn, New York 11235, USA*
[4]*Graduate School of Advanced Integration Science, Chiba University, 1-33 Yayoi-cho, Inage-ku, Chiba, 263-8522, Japan*
[5]*Dept. 1132, CINT, Sandia National Laboratories, MS 1303, Albuquerque, New Mexico 87185, USA*

(Received 26 October 2009; accepted 18 November 2009; published online 10 December 2009)

We demonstrate current-voltage spectroscopy of the one-dimensional subband structure of pinched-off quantum point contacts (QPCs). This technique yields the full subband structure and effective barrier of the QPC, without the need to perform an undesirable average over a range of gate voltage. Our measurements reveal strong asymmetry in the potential drop across the QPC, and a significantly enhanced subband spacing, in the pinch-off regime. © *2009 American Institute of Physics*. [doi:10.1063/1.3272677]

In quantum point contacts (QPCs), an important class of nanodevice, confinement is realized by applying a depleting voltage (V_g) to Schottky gates, forming a nanoconstriction that allows current flow via one-dimensional (1D) subbands.[1–3] The energy spacing of the subbands (Ξ) is related to the confinement, and can be determined from the differential conductance[4–7] [Fig. 1(a)]. For small source-drain bias (V_{sd}), conductance is quantized in units of $2e^2/h$.[2,3] For large V_{sd}, band bending causes the reservoirs to populate subbands unequally, leading to the appearance of "half-plateaus" once V_{sd} becomes comparable to Ξ.[4–7] While this approach has been used to determine Ξ,[8–20] it gives information only on the uppermost subband, and represents an average for a range of V_g (and confinement potentials). In this letter, we draw on classical point-contact spectroscopy[21] to quantify the subband structure of QPCs while avoiding these drawbacks. In point-contact spectroscopy, the connection of the second derivative of the current-voltage (I_d-V_{sd}) characteristic to the density of states has been exploited for materials characterization. By applying a model of harmonic saddle confinement in QPCs, we use the Landauer formalism[1] to calculate their I_d-V_{sd} characteristics. We show that structure in $\partial^2 I_d/\partial V_{sd}^2$ can provide a full spectroscopy of the QPC, yielding the effective height of the barrier at its center[1] and the energy separation of *successive* subbands. This information can be obtained in the pinch-off regime, in a single measurement that does not require any V_g average.

Current flow through a QPC is regulated by two features of its self-consistent potential, which grow more pronounced as the gate voltage is made stronger; a lateral confinement that quantizes the energy to form 1D subbands, and; a potential barrier in the direction of current flow that is driven through the Fermi level (E_F) when the QPC is pinched-off. This potential can be captured by assuming a harmonic saddlelike shape, for which the current (I_d) can be computed by summing over different 1D subbands[22]

$$I_d = \sum_n I_n, \quad I_n = \frac{2e^2}{h}\int_0^\infty [f(E) - f(E + eV_{sd})]T_n(E)dE. \tag{1}$$

Here, I_n is the contribution of the nth subband, $f(E)$ is the Fermi function, and T_n is the energy-dependent transmission coefficient

$$T_n(E) = [1 + \exp\{[(E_n + E_F) - E]/\delta_n\}]^{-1}. \tag{2}$$

In this expression, E_n is the height (relative to E_F) of the barrier seen by electrons in the n^{th} subband. This barrier is comprised of a "bare" part due to the saddle potential, and the subband energy. δ_n can be approximated as $(h/2\pi^2 L) \times [2(E_{n_o}+E_F)/m^*]^{0.5}$, where m^* is the electron effective mass, L is the QPC length, and E_{n_o} is the effective barrier height at $V_{sd}=0$. We take $E_{n_o}=e(V_{T_n}-V_g)/S$, where V_{T_n} is the gate voltage at which the effective barrier of the n^{th} subband crosses E_F and S is the gate-voltage lever arm, the conversion factor that relates changes of V_g to the associated shift of the QPC barrier. When $V_{sd}\neq 0$, the barrier height becomes $E_n=E_{n_o}\mp\alpha^{\pm}eV_{sd}$, where $\alpha^+(\alpha^-)$ is the fraction of V_{sd} dropped between the source (drain) and the top of the barrier when $V_{sd}>0(<0)$. For a symmetric QPC, $\alpha^+=\alpha^-=\frac{1}{2}$, but typically $\alpha^+\neq\alpha^-$ (Ref. 23) since the saddle point of the QPC barrier can be shifted toward either reservoir, dependent on the sign of V_{sd}.[24]

Figure 2(a) shows calculated I_d-V_{sd} curves at 1.45 K that span the open ($E_{1_o}<0$) and pinched-off ($E_{1_o}>0$) regimes. Motivated by experiment (below), we use $E_F=10$ meV, $V_{T_1}=-5.075$ V (for the lowest subband), $S=100$, $\alpha^+=0.28$, and $\alpha^-=0.13$. To calculate I_d, we consider six subbands with an equidistant spacing of 4.4 meV. For $V_g>-5.0$ V, the QPC is open and conducting at small V_{sd}, but for more-negative V_g it is pinched-off. In such cases, the QPC barrier decreases for all subbands as $|V_{sd}|$ is increased,[4–7] and this

a)Electronic mail: jbird@buffalo.edu.

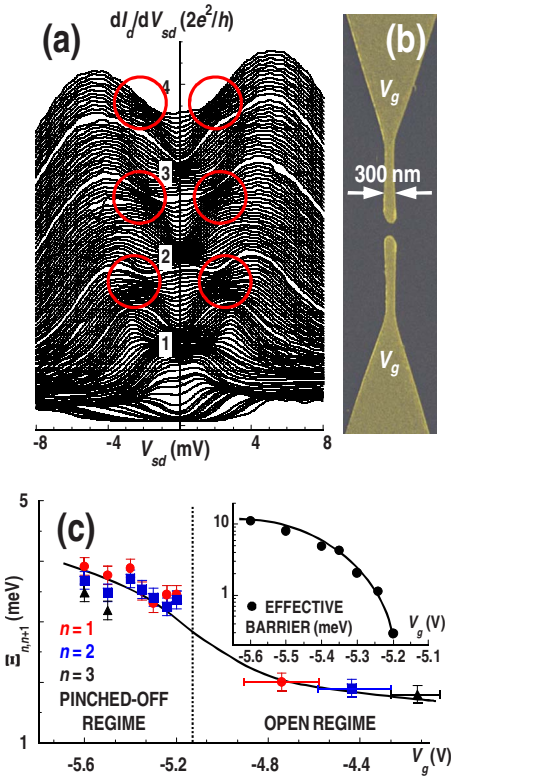

FIG. 1. (Color online) (a) Differential conductance of the QPC at 1.45 K. Different curves result from incrementing V_g in 15 mV steps from −5.24 to −4.12 V, from bottom to top, respectively. Circles identify half-integer bunching. (b) Electron micrograph of the QPC . (c) Main panel plots subband spacing vs V_g in the open and pinched-off regimes. Solid line is a guide to the eye. Horizontal error bars in the open regime indicate range of V_g average included for each data point. Inset: Effective barrier variation with V_g for the first subband.

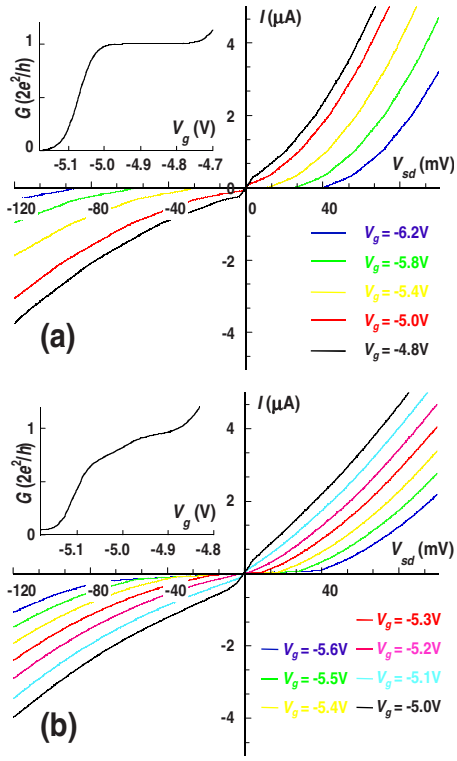

FIG. 2. (Color online) (a) Main panel shows calculated I_d-V_{sd} curves for different V_g and for the model parameters described in the text. The inset shows the calculated variation of conductance with V_g near V_{sd}=0. (b) Main panel shows measured I_d-V_{sd} curves for different V_g. The inset shows the variation of conductance with V_g measured near V_{sd}=0. Temperature is 1.45 K in (a) and (b).

causes the increase in current beyond some critical value $|V_c|$ [Fig. 2(a)]. Since $\alpha^+ \neq \alpha^-$, $|V_c|$ is different for positive and negative V_{sd}, and $|V_c|$ increases as V_g is made more negative and the local barrier in the QPC is raised.

The curves of Fig. 2(a) can be used to determine the barrier height and Ξ at any V_g. This is demonstrated by plotting $\partial^2 I_d/\partial V_{sd}^2$ versus V_{sd}, as in Fig. 3(a). This plot is for V_g=−6.2 V, and shows peaks that correspond to values of V_{sd} for which successive subbands cross E_F. Since α^+ is larger than α^-, implying positive V_{sd} more effectively moves the QPC barrier than negative V_{sd}, a larger number of subband openings is seen for positive V_{sd}. For either polarity, the first oscillation in $\partial^2 I_d/\partial V_{sd}^2$ occurs at V_c and allows E_{1_o} to be determined. In Fig. 3(a), for example, the model parameters yield E_{1_o}=11.25 meV, and we therefore have $V_c = E_{1_o}/\alpha^{\pm} e$ =+40 mV and −87 mV. As for the higher-order oscillations in Fig. 3(a), their spacing is given by $\Delta V_{sd} = \Xi/\alpha^{\pm} e$.

To explore our model we study the high-mobility GaAs/AlGaAs QPC (Sandia sample EA1278) of Fig. 1(b). This device was described in Ref. 25, and its two-dimensional electron gas density and mobility were 3.4×10^{11} cm^{-2} and 4×10^5 cm^2/Vs, respectively, at 2.5 K. Its differential conductance [Fig. 1(a)] shows standard curve bunching,[5] at integer plateaus near V_{sd}=0 and half plateaus (circled) at nonzero V_{sd}. The spacing of the n^{th} and $(n+1)$th subbands, $\Xi_{n,n+1}$ can be determined from this data for n=1, 2, and 3. These values are plotted in Fig. 1(c), in which error bars in V_g indicate the range over which $\Xi_{n,n+1}$ is averaged. We find $\Xi_{1,2}$=2 meV, $\Xi_{2,3}$=1.9 meV, and $\Xi_{3,4}$=1.8 meV, consis-

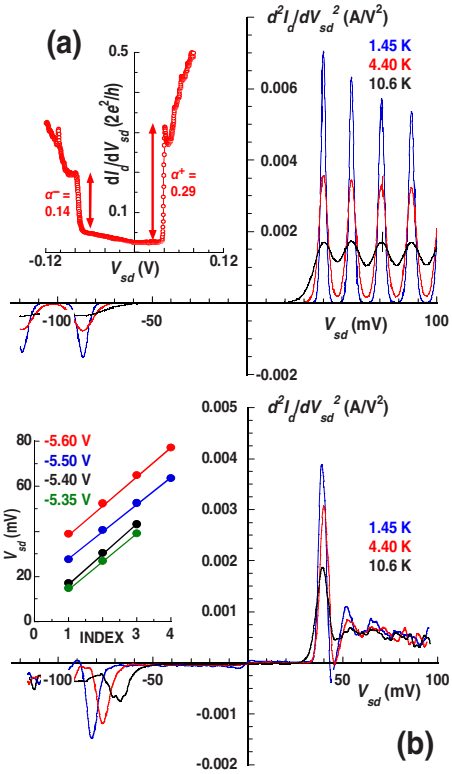

FIG. 3. (Color online) (a) Main panel shows calculated $\partial^2 I_d/\partial V_{sd}^2$ vs V_{sd} for the model parameters described in the text and for V_g=−6.20 V. Curves are shown for three different temperatures (indicated). The inset shows the differential conductance measured at 1.45 K for V_g=−5.60 V. (b) Main panel shows $\partial^2 I_d/\partial V_{sd}^2$ vs V_{sd}, at V_g=−5.60 V and three different temperatures (indicated). The inset plots the experimentally measured position of the oscillation peaks in $\partial^2 I_d/\partial V_{sd}^2$ for positive V_{sd} and for several V_g.

tent with increased confinement at more-negative V_g. We also determine the lever arm as $S=115$ mV/meV. The inset of Fig. 2(b) plots the QPC linear conductance ($V_{sd}=0.58$ mV), and shows the usual quantization and 0.7 feature.[1] The latter is not reproduced in our calculations, since it requires a many-body treatment.[1] The conductance plateau is noticeably wider in the numerical result [Fig. 2(a), inset], since the calculations take Ξ to be constant.

Figure 2(b) plots I_d-V_{sd} characteristics for our QPC at several V_g values and shows similar behavior to Fig. 2(a). When $V_g > -5.1$ V, the QPC is open at small V_{sd}, but, as V_g is made more negative, its barrier is driven above E_F and the I_d-V_{sd} curves develop strong nonlinearity. In Fig. 3(b), we plot $\partial^2 I_d/\partial V_{sd}^2$ for $V_g=-5.6$ V at three different temperatures and see many similarities with Fig. 3(a). Pronounced oscillations correspond to those predicted for the opening of successive subbands. The oscillation amplitude decreases with increasing temperature, similar to the theoretical curves. We use the features in $\partial^2 I_d/\partial V_{sd}^2$ to quantify the subband structure in the pinch-off regime.

We begin by determining α, which quantifies the voltage drop across the QPC. In Fig. 1(a), the half plateaus are close to 1.5, 2.5, and $3.5\times 2e^2/h$, for positive and negative V_{sd}, indicating V_{sd} is dropped symmetrically in this open regime $(\alpha^+=\alpha^-=\frac{1}{2})$.[5,6] At lower conductance the bunching occurs at 0.25 and $0.19\times 2e^2/h$ [Fig. 1(a)], implying $\alpha^+=0.25$ and $\alpha^-=0.19$. Such asymmetry has been noted in many experiments.[4,5,8,11,13] The α values can alternatively be determined from the I_d-V_{sd} curves by noting that, when V_{sd} is increased beyond V_c, a steplike increase from around zero to $\alpha^{\pm}2e^2/h$ should be seen in $\partial I_d/\partial V_{sd}$.[4] This is shown experimentally in the inset to Fig. 3(a), from which we determine $\alpha^+=0.29$ and $\alpha^-=0.14$. These values did not vary significantly with V_g in the pinch-off regime, and are similar to those obtained from the differential conductance [Fig. 1(a)].

With $\alpha^{\pm}$, we use $\partial^2 I_d/\partial V_{sd}^2$ to perform subband spectroscopy of the QPC. In the inset to Fig. 1(c), we show the V_g dependence of the effective barrier (E_{1_o}), as determined from $\alpha^{\pm}$ and V_c. The resulting variation is similar to that in Ref. 26 The period of the oscillations in $\partial^2 I_d/\partial V_{sd}^2$ should be directly related to the subband separation. In the inset to Fig. 3(b), we plot the V_{sd} position of the oscillations for several gate voltages. The data follow a linear dependence, implying a constant subband separation consistent with the harmonic approximation. In Fig. 1(c), we plot $\Xi_{n,n+1}$ and see that the values are significantly larger than for the open regime, consistent with enhanced confinement. As noted already, since $\alpha^+ > \alpha^-$, there are fewer oscillations at negative V_{sd} (see Fig. 3). Nonetheless, inferred values are found to be around 3.2–3.5 meV, consistent with positive polarity.

In Fig. 3(b), the oscillations are damped quickly with increasing V_{sd}, while for negative V_{sd} the position of the oscillation shifts with increasing temperature, features not found in the model. The reason for these differences is not clear at present, although they may reflect the role of hot-electron relaxation, neglected in our model.

In conclusion, we have demonstrated a spectroscopic technique, based on measurements of current-voltage characteristics, which allows the subband spacing and effective barrier in pinched-off QPCs to be determined.

Work supported by NSF (ECS-0609146), DoE (DE-FG03-01ER45920), and PSC-CUNY (62040-00 40) grants, and performed, in part, at the Center for Integrated Nanotechnologies, a U.S. DoE Office of Basic Energy Sciences nanoscale science research center. Sandia National Laboratories is a multiprogram laboratory operated by Sandia Corporation, a Lockheed–Martin Co., for the U.S. DoE (Contract No. DE-AC04-94AL85000).

[1] D. K. Ferry, S. M. Goodnick, and J. P. Bird, *Transport in Nanostructures*, 2nd ed. (Cambridge University Press, Cambridge, U.K., 2009).
[2] D. A. Wharam, T. J. Thornton, R. Newbury, M. Pepper, H. Ahmed, J. E. F. Frost, D. G. Hasko, D. C. Peacock, D. A. Ritchie, and G. A. C. Jones, J. Phys. C **21**, L209 (1988).
[3] B. J. van Wees, H. van Houten, C. W. J. Beenakker, J. G. Williamson, L. P. Kouwenhoven, D. van der Marel, and C. T. Foxon, Phys. Rev. Lett. **60**, 848 (1988).
[4] L. P. Kouwenhoven, B. J. van Wees, C. J. P. M. Harmans, J. G. Williamson, H. van Houten, C. W. J. Beenakker, C. T. Foxon, and J. J. Harris, Phys. Rev. B **39**, 8040 (1989).
[5] N. K. Patel, J. T. Nicholls, L. Martin-Moreno, M. Pepper, J. E. F. Frost, D. A. Ritchie, and G. A. C. Jones, Phys. Rev. B **44**, 13549 (1991).
[6] L. I. Glazman and A. V. Khaetskii, Europhys. Lett. **9**, 263 (1989).
[7] A. M. Zagoskin, JETP Lett. **52**, 436 (1990).
[8] T. Heinzel, D. A. Wharam, F. M. de Aguiar, J. P. Kotthaus, G. Böhm, W. Klein, G. Tränkle, and G. Weimann, Semicond. Sci. Technol. **9**, 1220 (1994).
[9] K. J. Thomas, M. Y. Simmons, J. T. Nicholls, D. R. Mace, M. Pepper, and D. A. Ritchie, Appl. Phys. Lett. **67**, 109 (1995).
[10] A. J. Daneshvar, C. J. B. Ford, A. R. Hamilton, M. Y. Simmons, M. Pepper, and D. A. Ritchie, Phys. Rev. B **55**, R13409 (1997).
[11] A. Kristensen, H. Bruus, A. E. Hansen, J. B. Jensen, P. E. Lindelof, C. J. Marckmann, J. Nygård, C. B. Sørensen, F. Beuscher, A. Forchel, and M. Michel, Phys. Rev. B **62**, 10950 (2000).
[12] S. M. Cronenwett, H. J. Lynch, D. Goldhaber-Gordon, L. P. Kouwenhoven, C. M. Marcus, K. Hirose, N. S. Wingreen, and V. Umansky, Phys. Rev. Lett. **88**, 226805 (2002).
[13] D. J. Reilly, T. M. Buehler, J. L. O'Brien, A. R. Hamilton, A. S. Dzurak, R. G. Clark, B. E. Kane, L. N. Pfeiffer, and K. W. West, Phys. Rev. Lett. **89**, 246801 (2002).
[14] L. Worschech, D. Hartmann, S. Reitzenstein, and A. Forchel, J. Phys.: Condens. Matter **17**, R775 (2005).
[15] S. F. Fischer, G. Apetrii, U. Kunze, D. Schuh, and G. Abstreiter, Nat. Phys. **2**, 91 (2006).
[16] R. Danneau, O. Klochan, W. R. Clarke, L. H. Ho, A. P. Micolich, M. Y. Simmons, A. R. Hamilton, M. Pepper, D. A. Ritchie, and U. Zulicke, Phys. Rev. Lett. **97**, 026403 (2006).
[17] O. Gunawan, B. Habib, E. P. De Poortere, and M. Shayegan, Phys. Rev. B **74**, 155436 (2006).
[18] T. P. Martin, A. Szorkovszky, A. P. Micolich, A. R. Hamilton, C. A. Marlow, H. Linke, R. P. Taylor, and L. Samuelson, Appl. Phys. Lett. **93**, 012105 (2008).
[19] T.-M. Chen, A. C. Graham, M. Pepper, F. Sfigakis, I. Farrer, and D. A. Ritchie, Phys. Rev. B **79**, 081301(R) (2009).
[20] K. Gloos, P. Utko, M. Aegesen, C. B. Sorenson, J. Bindslev Hansen, and P. E. Lindelof, Phys. Rev. B **73**, 125326 (2006).
[21] A. M. Duif, A. G. M. Jansen, and P. Wyder, J. Phys.: Condens. Matter **1**, 3157 (1989).
[22] H. A. Fertig and B. I. Halperin, Phys. Rev. B **36**, 7969 (1987).
[23] H. van Houten, C. W. J. Beenakker, and B. J. van Wees, *Semiconductors and Semimetals*, edited by M. A. Reed (Academic, New York, 1992), Vol. 35, pp. 35–112.
[24] K. S. Novoselov, Yu. V. Dubrovskii, V. A. Sablikov, D. Yu. Ivanov, E. E. Vdovin, Yu. N. Khanin, V. A. Tulin, D. Esteve, and S. Beaumont, Europhys. Lett. **52**, 660 (2000).
[25] J. W. Song, N. A. Kabir, Y. Kawano, K. Ishibashi, G. R. Aizin, L. Mourokh, J. L. Reno, A. G. Markelz, and J. P. Bird, Appl. Phys. Lett. **92**, 223115 (2008).
[26] A. Ramamoorthy, J. P. Bird, and J. L. Reno, Appl. Phys. Lett. **89**, 013118 (2006).